Exciton-phonon interaction in fractional dimensional space

A. Thilagam
Faculty of Science, Northern Territory University, Northern Territory 0909, Australia
(Received 30 April 1997)

Explicit analytical expressions of Frohlich-like Hamiltonians for the interaction between an exciton and optical phonons in fractional-dimensional space are derived for two illustrative cases of $1s\rightarrow 1s$ and $1s\rightarrow 2p$ exciton scattering. The improved Hamiltonians incorporate any modification in the strength of the exciton-optical-phonon interactions due to confinement, by means of a single parameter α, a measure of the dimensionality of the confined system. The Hamiltonians also incorporate the penetration of electron and hole wave functions into the barrier region, an effect which becomes increasingly significant for narrow well widths. The flexibility of the derived Hamiltonians are shown in the ease of systematic study of exciton linewidths in $GaAs/Al_xGa_{1-x}As$ quantum wells. Results show the high sensitivity of the excitonic linewidths to α due to interactions with short-wavelength optical phonons. [S0163-1829(97)01139-9]

I. INTRODUCTION

Interactions involving excitons and phonons play an important role in the properties of quantum wells and superlattices[1–3] as the emission and absorption spectra near the band-gap region is dominated by excitonic features[4] in high quality semiconductors. Earlier works[5–8] have generally used an exact three-dimensional or two-dimensional Hamiltonians to study the exciton-optical-phonon interaction in quantum wells. The form of these Hamiltonians are inflexible and can only model the exciton-optical-phonon interaction rather approximately. Studies[9,10] of the exciton-optical-phonon interaction in $GaAs/Al_xGa_{1-x}As$ and $GaAs/In_xGa_{1-x}As$ single quantum wells have shown that the main phonon modes involved in the exciton-phonon interaction are neither the two-dimensional type as in the case of confined phonons or the three-dimensional phonons common in bulk phonon modes. There are a variety of phonon modes which arises from the anisotropy of quantum wells, which have been described by the Huang and Zhu model, Fuchs-Kliewer slab modes or Ridley's guided mode models.[10–12] These phonon modes undergo a gradual change in dimensionality as the well width varies from zero to infinity.

The pseudo-two-dimensionality behavior of excitons in quantum wells was first popularized by He *et al.*[13] and Lefebvre *et al.*[14–16] Their use of fractional-dimensional space greatly simplified the problem of solving the energy levels of excitons in quantum well structures. In our work here, we present a unified approach to exciton-phonon interaction in quantum wells by treating both the exciton and phonons as existing in fractional-dimensional space. The exciton-optical-phonon interaction operators are derived in a fractional-dimensional space, as a result, the interaction operators are modified accordingly with changes in the quantum well width. The main advantage in using a fractional-dimensional space is that only a single parameter, known as the degree of dimensionality (denoted by α), is needed to incorporate the effects due to changes in the widths of the well or barrier regions on the strength of exciton-phonon interaction as α increases from 2 in an exact two-dimensional system (e.g., infinite potential with zero well width) to 3 in an exact three-dimensional system (zero confinement). Our results shows that the dimensionality, α, is a critical factor in the interaction between exciton and short-wavelength optical phonons.

This paper is organized as follows. In Sec. II, we define an α-dimensional electron-phonon interaction involving longitudinal-optical phonons. We also present the derivation of the α-dimensional exciton-phonon matrix elements for $1s\rightarrow 1s$ and $1s\rightarrow 2p$ scattering. In Sec. III, we study the effect of dimensionality on exciton-optical-phonon interaction and analyze the behavior of the interaction operators derived in Sec. II, in the small wavevector limit. In Sec. IV, we obtain obtain numerical results of the exciton linewidth in $GaAs/Al_xGa_{1-x}As$ quantum wells and present the conclusion of this work in Sec. V.

II. EXCITON-OPTICAL-PHONON INTERACTION IN A FRACTIONAL-DIMENSIONAL SPACE

We define the α-dimensional electron-phonon interaction involving longitudinal-optical phonons by the Fröhlich type Hamiltonian:

$$H_{\text{ex-ph}}^{\text{op }\alpha\text{D}}=\sum_{\mathbf{K},\mathbf{q},\lambda,\nu} V_{\lambda,\nu}^{\alpha}(\mathbf{q})B_{\mathbf{K}+\mathbf{q},\nu}^{\dagger}B_{\mathbf{K},\lambda}(b_q+b_q^{\dagger}), \qquad (1)$$

where the exciton operators $(B_{\mathbf{K}}^{\dagger},B_{\mathbf{K}})$, and phonon operators $(b_q,b_q^{\dagger})$ are considered to operate in a fractional-dimensional space. All position $(\mathbf{r})$ and momentum vectors $(\mathbf{K},\mathbf{q})$ are taken to exist in a fractional-dimensional space.

λ and ν in Eq. (1) are the internal quantum numbers of the exciton state and the matrix element, $V_{\lambda,\nu}^{\alpha}(\mathbf{q})$, in αD space is given by

$$V_{\lambda,\nu}^{\alpha}(\mathbf{q})=\int_{\alpha\text{D}} d\mathbf{r}\ \psi_{\nu}^{\dagger}(\mathbf{r})\psi_{\lambda}(\mathbf{r})V_{\mathbf{q}}^{\alpha}[\exp(-\mathbf{i}\gamma_e\mathbf{q}\cdot\mathbf{r_e}) - \exp(\mathbf{i}\gamma_h\mathbf{q}\cdot\mathbf{r_h})], \qquad (2)$$

where

$$\gamma_e=\frac{m_e^*}{(m_e^*+m_h^*)} \quad \text{and} \quad \gamma_h=\frac{m_h^*}{(m_e^*+m_h^*)} \tag{3}$$

and

$$|V_{\mathbf{q}}^{\alpha}|^2=\frac{2\pi e^2\hbar\omega_{\mathrm{LO}}}{\Omega^{\alpha}q^{\alpha-1}}\left(\frac{1}{\varepsilon_{\infty}}-\frac{1}{\varepsilon_0}\right), \tag{4}$$

where ε_{∞} and ε_0 are the high- and low-frequency values of the dielectric function of the well material. m_e^* and m_h^* are the respective electron and hole band masses and ω_{LO} is the frequency of the LO phonons. In Eq. (4), we have neglected the LO-phonon dispersion by assuming that $\hbar\omega_{\mathrm{LO}}(\mathbf{q})\approx\hbar\omega_{\mathrm{LO}}(0)$. Ω^{α} in Eq. (4) is the volume in an αD space, which is given by the Hausdorff measure,

$$\Omega^{\alpha}(|\mathbf{r}|)=\frac{\pi^{\alpha/2}}{\Gamma\left[1+\frac{\alpha}{2}\right]}|\mathbf{r}|^{\alpha} \tag{5}$$

where $\Gamma[x]$ is the Euler's Γ function. Note that we have generalized Eq. (4) by introducing a noninteger dimension α. Equation (4) reduces to the well established forms in both the exact 2D and 3D limits.

Instead of involved derivation of the exciton-optical-phonon interaction operator for all allowed exciton states, we only consider two important cases: (1) $\lambda=\nu=1s$ (intraband scattering) and (2) $\lambda=1s$, $\nu=2p$ (interband scattering). This is justified as in energy transitions involving excitonic states, only the $1s$ exciton states[17] are considered since they have a much stronger coupling to the photons than higher order states as the excitonic oscillator strength falls as $\sim 1/n^3$. The quantum number, $n=1,2,\ldots$ is the principal quantum number state of the exciton. We have included the case of $\lambda=1s$, $\nu=2p$ for the purpose of comparison with $\lambda=\nu=1s$. In general, the two cases we study here are sufficient to account for the salient features of exciton based transitions in resonant Raman scattering experiments.[17]

The $1s$ state of an exciton in an αD space, which is needed in both cases, can be written as

$$\psi_{1s}(r)=F(\alpha)\exp\left[-\frac{2}{\alpha-1}\frac{r}{a_B}\right], \tag{6}$$

where a_B is the three-dimensional Bohr radius of the exciton. Likewise, the wave function of a $2p$-state exciton in an αD space can be written as

$$\psi_{2p}(r)=G(\alpha)\frac{r}{a_B}\exp\left[-\frac{2}{\alpha+1}\frac{r}{a_B}\right]\cos\theta, \tag{7}$$

where $F(\alpha)$ and $G(\alpha)$ in Eqs. (6) and (7) can be easily obtained as

$$F(\alpha)=\left[\frac{2^{\alpha+1}\pi^{(1-\alpha)/2}}{\Gamma\left[\frac{\alpha-1}{2}\right](\alpha-1)^{\alpha+1}}\frac{1}{a_B^{\alpha}}\right]^{1/2} \tag{8}$$

and

$$G(\alpha)=\left[\frac{2^{\alpha+4}\pi^{(1-\alpha)/2}}{\Gamma\left[\frac{\alpha+1}{2}\right](\alpha+1)^{3+\alpha}}\frac{1}{a_B^{\alpha}}\right]^{1/2}. \tag{9}$$

It is important to note that we have specifically chosen a $2p$ exciton state for which the quantum number, $m=0$, in Eq. (7). Because of the axial symmetry of the operator terms, $e^{(-\mathbf{i}\gamma_e\mathbf{q}\cdot\mathbf{r_e})}$ and $e^{(\mathbf{i}\gamma_h\mathbf{q}\cdot\mathbf{r_h})}$ which appear in Eq. (2), only exciton scattering in which m is conserved, is allowed

Using the relation[18,19]

$$\int_{\alpha D}d\mathbf{r}\;e^{-2\pi|\mathbf{r}|c}e^{-2\pi\mathbf{i}\mathbf{q}\cdot\mathbf{r}}=\frac{\Gamma\left[\frac{\alpha+1}{2}\right]}{\pi^{(\alpha+1)/2}}\;\frac{c}{(c^2+q^2)^{(\alpha+1)/2}} \tag{10}$$

and the hydrogenic form of the wave function, ψ_{1s} in αD space given in Eq. (6), the matrix element, $V_{1s,1s}^{\alpha}(\mathbf{q})$ in Eq. (2) can be evaluated as

$$\begin{aligned}V_{1s,1s}^{\alpha}(\mathbf{q})=&\left(\frac{2\pi e^2\hbar\omega_{\mathrm{LO}}}{\Omega^{\alpha}q^{\alpha-1}}\right)^{1/2}\\&\times\left(\frac{1}{\varepsilon_{\infty}}-\frac{1}{\varepsilon_0}\right)^{1/2}\\&\times\left[\frac{1}{[1+\beta_h^2(\alpha)]^{(\alpha+1)/2}}\right.\\&\left.-\frac{1}{[1+\beta_e^2(\alpha)]^{(\alpha+1)/2}}\right],\end{aligned} \tag{11}$$

where

$$\beta_h(\alpha)=\frac{\gamma_h|\mathbf{q}|}{2}\left(\frac{\alpha-1}{2}\right)a_B$$

and

$$\beta_e(\alpha)=\frac{\gamma_e|\mathbf{q}|}{2}\left(\frac{\alpha-1}{2}\right)a_B. \tag{12}$$

It is to be noted that Eq. (10) is based on functions known as the Poisson kernal which are discussed in detail by Stein and Weiss.[19] In deriving Eq. (11), we have made use of the spatial integral relation in αD space:[13]

$$\int_{\alpha D}dr=\frac{2\pi^{(\alpha-1)/2}}{\Gamma\left[\frac{\alpha-1}{2}\right]}\int_0^{\infty}r^{\alpha-1}dr\int_0^{\pi}d\theta\,\sin^{\alpha-2}\theta. \tag{13}$$

The derivation of the matrix element, $V_{1s,2p}^{\alpha}(\mathbf{q})$ involves the use of the integral (see Appendix A):

$$\begin{aligned}&\frac{1}{|q|}\int_{\alpha D}d\mathbf{r}\;\mathbf{q}\cdot\mathbf{r}e^{-2\pi|\mathbf{r}|c}e^{-2\pi\mathbf{i}\mathbf{q}\cdot\mathbf{r}}\\&=\frac{\Gamma\left[\frac{\alpha+3}{2}\right]}{\pi^{(\alpha+3)/2}}\frac{\mathbf{i}cq}{(c^2+q^2)^{(\alpha+3)/2}}.\end{aligned} \tag{14}$$

Using Eqs. (2), (6), (7), and (14), the matrix element, $V^{\alpha}_{1s,2p}(\mathbf{q})$ in Eq. (2) can be evaluated as

$$V^{\alpha}_{1s,2p}(\mathbf{q})=\left(\frac{2\pi e^2\hbar\omega_{\mathrm{LO}}}{\Omega^{\alpha}q^{\alpha-1}}\right)^{1/2}\left(\frac{1}{\varepsilon_{\infty}}-\frac{1}{\varepsilon_0}\right)^{1/2}V(\alpha)(a_Bq)\times\left[\frac{\gamma_h}{[1+\xi_h^2(\alpha)]^{(\alpha+3)/2}}-\frac{\gamma_e}{[1+\xi_e^2(\alpha)]^{(\alpha+3)/2}}\right], \tag{15}$$

where

$$\xi_h(\alpha)=\frac{\gamma_h|\mathbf{q}|}{2}P(\alpha)a_B \quad \text{and} \quad \xi_e(\alpha)=\frac{\gamma_e|\mathbf{q}|}{2}P(\alpha)a_B \tag{16}$$

and

$$P(\alpha)=\left(\frac{\alpha^2-1}{2\alpha}\right) \tag{17}$$

and $V(\alpha)$ can be easily obtained using Eqs. (8) and (9) as

$$V(\alpha)=\frac{2^{\alpha}P^{\alpha+1}(\alpha)}{(\alpha^2-1)^{\alpha/2}(\alpha+1)^{1/2}}. \tag{18}$$

The matrix elements, $V^{\alpha}_{1s,1s}(\mathbf{q})$ and $V^{\alpha}_{1s,2p}(\mathbf{q})$ both yield the expected forms[5–8] in the exact three-dimensional and two-dimensional limits. The matrix elements also vanish for $m_e^*=m_h^*$. Experimental results[20] confirm this behavior for excitons in bulk.[20] We are unable to find existing experimental results showing this result for excitons in quantum wells.

III. EFFECT OF DIMENSIONALITY ON EXCITON-OPTICAL-PHONON INTERACTION

The dependency of the Hamiltonian, $H^{\mathrm{op}\ \alpha\mathrm{D}}_{\text{ex-ph}}$ on the phonon wave vector, $\mathbf{q}$, is critically determined by the symmetry of the the initial and final exciton states. For states of the same parity, i.e., $\lambda=\nu=1s$, $H^{\mathrm{op}\ \alpha\mathrm{D}}_{\text{ex-ph}}\to 0$ as $|\mathbf{q}|\to 0$. This holds true for $2\leqslant\alpha\leqslant 3$. For states of different parity, i.e., $\lambda=1s$, $\nu=2p$, $H^{\mathrm{op}\ \alpha\mathrm{D}}_{\text{ex-ph}}\to 0$ as $|\mathbf{q}|\to 0$ for all values of α less than 3. However $H^{\mathrm{op}\ \alpha\mathrm{D}}_{\text{ex-ph}}$ takes on a finite value at $\alpha=3$. The behavior of $H^{\mathrm{op}\ \alpha\mathrm{D}}_{\text{ex-ph}}$ at $\mathbf{q}=\mathbf{0}$ is consistent with that obtained for the exact three-dimensional system by Bulyanitsa *et al.*[21]

Figure 1 shows a plot of the matrix element term, $\langle 1s|H^{\mathrm{op}\ \alpha\mathrm{D}}_{\text{ex-ph}}|1s\rangle$:

$$\langle 1s|H^{\mathrm{op}\ \alpha\mathrm{D}}_{\text{ex-ph}}|1s\rangle \sim \frac{1}{(a_B|\mathbf{q}|)^{(\alpha-1)/2}}\left[\frac{1}{[1+\beta_h^2(\alpha)]^{(\alpha+1)/2}}-\frac{1}{[1+\beta_e^2(\alpha)]^{(\alpha+1)/2}}\right] \tag{19}$$

as a function of $a_B|\mathbf{q}|$ for different values of α. We have chosen values of $\gamma_e=0.3$ and $\gamma_h=0.7$ appropriate for a $GaAs/Al_xGa_{1-x}As$ system. The matrix element, in Fig. 1, increases gradually to a broad maximum at $q_{\max}$, before decreasing again. The stength of the exciton-phonon interaction

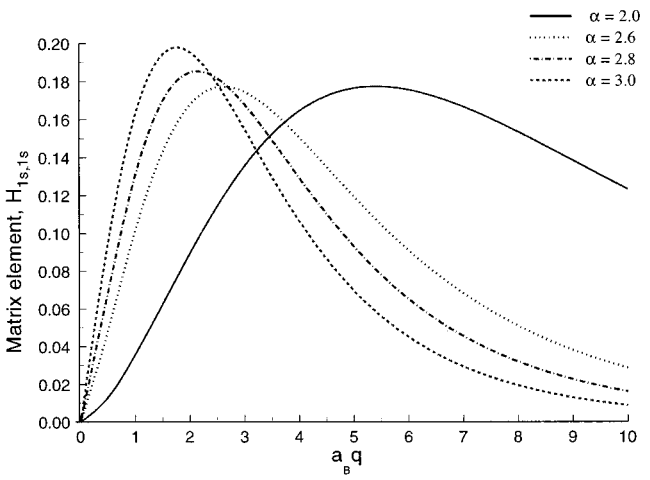

FIG. 1. Plot of the matrix element term, $\langle 1s|H^{\mathrm{op}\ \alpha\mathrm{D}}_{\text{ex-ph}}|1s\rangle$ as a function of $(a_B|\mathbf{q}|)$ at different values of α.

for $1s\to 1s$ scattering increases with α while $q_{\max}$ decreases with α. The width of the maximum can generally be seen to decrease with the dimensionality of the quantum well.

In Fig. 2, we have plotted $\langle 1s|H^{\mathrm{op}\ \alpha\mathrm{D}}_{\text{ex-ph}}|1s\rangle$ in Eq. (19), as a function of α for different values of $a_B|\mathbf{q}|$. The matrix element remains unaffected by α for $a_B|\mathbf{q}|\sim 3$, however for $a_B|\mathbf{q}|\leqslant 3$ it decreases with α, while the reverse occurs for $a_B|\mathbf{q}|\geqslant 3$.

Figure 3 shows a plot of the matrix element term, $\langle 1s|H^{\mathrm{op}\ \alpha\mathrm{D}}_{\text{ex-ph}}|2p\rangle$:

$$\langle 1s|H^{\mathrm{op}\ \alpha\mathrm{D}}_{\text{ex-ph}}|2p\rangle \sim \frac{V^2(\alpha)}{(a_B|\mathbf{q}|)^{(\alpha-3)/2}}\left[\frac{\gamma_h}{[1+\xi_h^2(\alpha)]^{(\alpha+3)/2}}-\frac{\gamma_e}{[1+\xi_e^2(\alpha)]^{(\alpha+3)/2}}\right] \tag{20}$$

as a function of $|\mathbf{q}|a_B$ for different values of α. As in Eq. (19), we have used $\gamma_e=0.3$ and $\gamma_h=0.7$. Unlike in the case of $1s\to 1s$ scattering, the matrix element, $V_{1s,2p}$ has maxima peaks at two different values of the phonon wave vector.

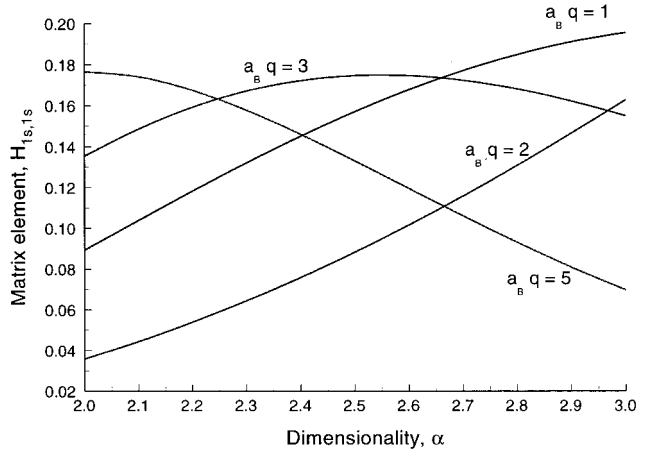

FIG. 2. Plot of the matrix element term, $\langle 1s|H^{\mathrm{op}\ \alpha\mathrm{D}}_{\text{ex-ph}}|1s\rangle$ as a function of α at different values of $(a_B|\mathbf{q}|)$.

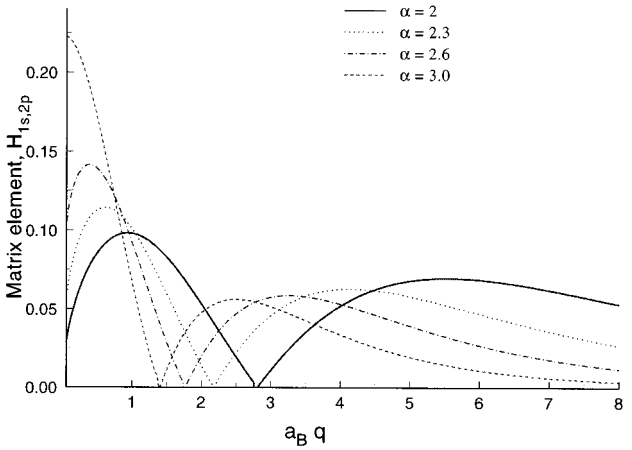

FIG. 3. Plot of the matrix element term, $\langle 1s|H_{\text{ex-ph}}^{\text{op }\alpha\text{D}}|2p\rangle$ as a function of $(a_B|\mathbf{q}|)$ at different values of α.

After the first maximum, $\langle 1s|H_{\text{ex-ph}}^{\text{op }\alpha\text{D}}|2p\rangle$ reaches zero for values of phonon wave vector, q_c, given by

$$q_c=\frac{1}{P(\alpha)}\left[\frac{\left(\frac{\gamma_h}{\gamma_e}\right)^{[2/(\alpha+3)]-1}}{\left(\frac{\gamma_h}{2}\right)^2-\left(\frac{\gamma_h}{\gamma_e}\right)^{2/(\alpha+3)}\left(\frac{\gamma_e}{2}\right)^2}\right]^{1/2}. \tag{21}$$

Equation (21) shows that as α decreases, q_c increases for fixed values of γ_e and γ_h, as is shown in Fig. 3.

The exciton-phonon interaction operators in Eqs. (19) and (20) yield different expressions for the two- and three-dimensional cases due to different powers in terms of $[1+\beta_i^2(\alpha)]$ and $[1+\xi_i^2(\alpha)]$ $(i=e,h)$. There is little difference between the exact two-dimensional and three-dimensional behavior of the interaction operators, $V_{1s,1s}^{\alpha}(\mathbf{q})$ and $V_{1s,2p}^{\alpha}(\mathbf{q})$, for long-wavelength phonons where β_i and ξ_i can be neglected. However, for short-wavelength phonons, the differences would be significant as is shown in Figs. 1–3, and is expected to give rise to major differences in the transport properties of excitons in quasi-two-dimensional systems.

A. Cancellation effect at small phonon wave vectors

It is important to analyze the salient features of the matrix elements, $V_{1s,1s}$ and $V_{1s,2p}$ for small values of the wave vector, q near the origin. In an ideal semiconductor, the exciton center of mass wave vector equals zero as the excitation is caused by an optical photon which does not occur in practice due to several mechanisms.[22,23] Thus the dependence of the Fröhlich exciton-optical phonon matrix element on q is important in resonant Raman scattering studies.[24] The interaction of a longitudinal-optical phonon with an excitonic state becomes highly enhanced, when an incident photon becomes resonant with the initial, $1s$ state. As shown in Figs. 1 and 3, the strong dependency on q, gives rise to a different set of Raman rules[25] which are not based on $q\approx 0$.

In the Fröhlich type exciton-phonon interaction, the electrostatic interaction term, $V_{\mathbf{q}}^{\alpha}$ in Eq. (4) remains the same for both the conduction and valence bands in contrast to the deformation potential interaction which differs from band to band. This accounts for the cancellation effect of $1s\rightarrow 1s$ scattering for small values of q. Physically, this means that for large wavelength phonons, the exciton is ''seen'' as electrically neutral which results is almost zero coupling. For small values of $\mathbf{q}$, Eq. (19) reduces to

$$\langle 1s|H_{\text{ex-ph}}^{\text{op }\alpha\text{D}}|1s\rangle\sim\left(\frac{m_e^*-m_h^*}{m_e^*+m_h^*}\right)(a_B|\mathbf{q}|), \tag{22}$$

hence if $m_h^*\gg m_e^*$, the cancellation effect becomes less significant at small $\mathbf{q}$'s. Due to the mixing of different states of relative motion, the cancellation effect at small phonon wave vectors is less significant for the $1s\rightarrow 2s$ scattering, and is strongly dependent on the dimensionality of the exciton.

B. Determining dimensionality, α, of an exciton in a quantum well

It is important to use a proper definition for the dimensionality of the confined exciton in order to obtain accurate values of α. Mathieu *et al.*[14] have suggested a simple defination by which α can be easily computed for a given value of the well width:

$$\alpha_{\text{ex}}=3-\exp\left(-\frac{L_w}{2a_{\text{ex}}}\right), \tag{23}$$

where L_w is the well width and a_{ex} is the exciton bohr radius.

In general, reliable values of α of an exciton in a quantum well of known well width can be obtained by using experimental values[26] of exciton binding energies as a function of the well width. The dimensionality is then determined by using a simple expression[13,14] of the exciton energy, E_b:

$$E_b=\frac{R_y}{\left(n+\frac{\alpha-3}{2}\right)^2}, \tag{24}$$

where the quantum number, $n=1,2,\ldots$ is the principal quantum number state and R_y is the effective Rydberg. The empirical estimates of α are generally larger by 0.15–0.20 than the values calculated using Eq. (23). This is mainly attributed to the fact that Eq. (24) is an exact result of the exciton binding energy whereas Eq. (23) is based on an empirical assumption.[14]

In Fig. 4, we have plotted α of the heavy-hole exciton as a function of the well width using empirical values of exciton binding energies[26] in GaAs/Al_xGa_{1-x}As quantum wells. It can be seen that the ideal confinement at which $\alpha=2$ is never reached[27,28] due to the spreading of electron and hole wave functions into the barrier regions. It is important to note that this spreading effect, which becomes significant for thin wells, is taken into account in the matrix elements, Eq. (19) and Eq. (20), through α.

IV. EXCITON LINEWIDTHS IN GaAs/Al_xGa_{1-x}As QUANTUM WELLS

Studies of the exciton linewidth[29] is important as it primarily determines the shape of the absorption spectra. At room temperatures, the exciton-optical-phonon scattering dominates[6] over scattering processes involving acoustic

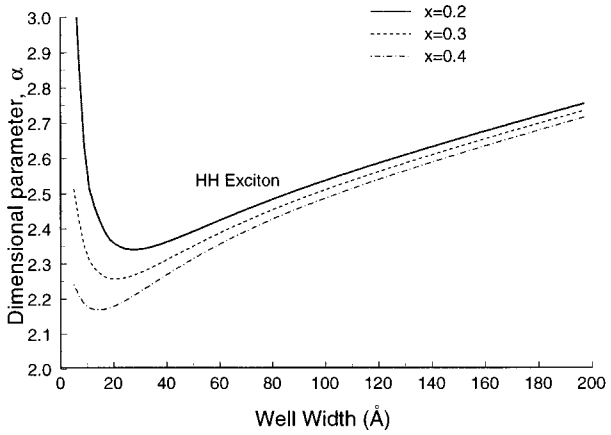

FIG. 4. Dimensionality, α, of the heavy-hole exciton, as a function of well width at various aluminum concentration, x in $GaAs/Al_xGa_{1-x}As$ quantum wells.

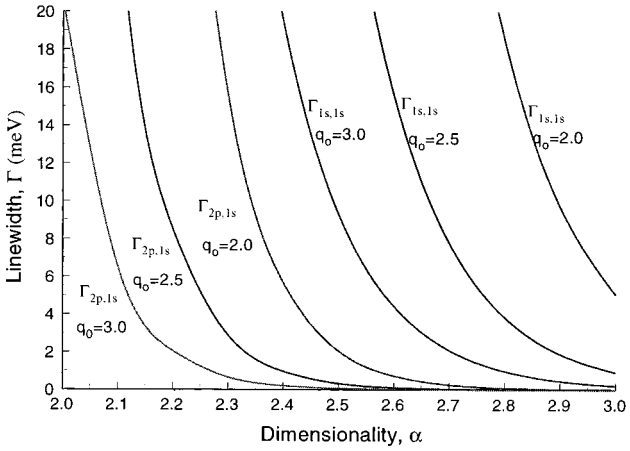

FIG. 5. Exciton linewidths, $\Gamma_{1s,1s}$ and $\Gamma_{2p,1s}$ as a function of dimensionality, α at $q_0=2$, 2.5, and 3 [see Eq. (29)].

phonons. Since the optical-phonon energy, $\hbar\omega_{\mathrm{LO}}$, is larger than the binding energy of an exciton, it is highly likely that the exciton decays to the continuum state after collision with an optical phonon. However it also possible for the exciton to jump to the excited $2s$ or higher states, with an increase in the kinetic energy in its center-of-mass motion.

For the purpose of simplicity in analytical expressions, we shall assume that the final states in the exciton-optical-phonon interaction are in the $1s$ or $2p$ state. This possibility cannot be excluded for hot excitons[30,31] in which the kinetic energy is large enough to be of the same order as the binding energy.

Using Eqs. (1) and (11), the magnitude of the exciton linewidth due to $1s\rightarrow 1s$ scattering by optical phonons can be obtained as

$$\Gamma_{1s,1s}=\left(\frac{2\pi e^2\hbar\omega_{\mathrm{LO}}}{\Omega^{\alpha}}\right)\left(\frac{1}{\varepsilon_\infty}-\frac{1}{\varepsilon_0}\right)\sum_{\mathbf{q}}\ \frac{1}{q^{\alpha-1}} \times\left[\frac{1}{[1+\beta_h^2(\alpha)]^{(\alpha+1)/2}}-\frac{1}{[1+\beta_e^2(\alpha)]^{(\alpha+1)/2}}\right]^2 \times\delta[\hbar\omega-E_{1s}(\mathbf{q})+\hbar\omega_{\mathrm{LO}}]. \tag{25}$$

The δ function in Eq. (25) conserves the energy of the scattered exciton and phonon in the αD space. $E_{1s}(\mathbf{q})$ denotes the energy of the $1s$ exciton and the phonon wave vector, $|\mathbf{q}|$, is restricted to the range

$$K-\left(K^2-\frac{2M\omega_{\mathrm{LO}}}{\hbar}\right)^{1/2}\leqslant q\leqslant K+\left(K^2-\frac{2M\omega_{\mathrm{LO}}}{\hbar}\right)^{1/2}, \tag{26}$$

where $M=m_e^*+m_h^*$ is the total mass of the exciton and K is the exciton wave vector.

Transforming the discrete sum over the phonon wave vectors, $\mathbf{q}$, in Eq. (25) into a spatial integral using

$$\sum_{\mathbf{q}}\ \rightarrow\frac{\Omega^{\alpha}}{(2\pi)^{\alpha}}\int_{\alpha\mathrm{D}}d\mathbf{q}, \tag{27}$$

we get a simple expression for the exciton linewidth, $\Gamma_{1s,1s}$, in meV as

$$\Gamma_{1s,1s}(q_0)=2.7\times10^5\ \frac{1}{(2\pi)^{\alpha-1}q_0}\left[\frac{1}{[1+\beta_h(\alpha)^2]^{(\alpha+1)/2}}-\frac{1}{[1+\beta_e(\alpha)^2]^{(\alpha+1)/2}}\right]^2, \tag{28}$$

where the dimensionless wave vector, q_0, is given by

$$q_0=L_0|\mathbf{q}|=\frac{2ML_0}{\hbar^2}\,[\hbar\omega-E_{1s}(\mathbf{q})+\hbar\omega_{\mathrm{LO}}], \tag{29}$$

where $L_0=\sqrt{(\hbar/2m_e^*\omega_{\mathrm{LO}})}$ and the exact value of the dimensionless wave vector, q_0, depends on the photon energy, $\hbar\omega$, the exciton energy, $E_{1s}(\mathbf{q})$, and the range imposed by the conservation law given in Eq. (26).

Likewise an expression for the exciton linewidth, $\Gamma_{2p,1s}$, in meV, can be obtained using Eqs. (1) and (15) as

$$\Gamma_{2p,1s}=1.3\times10^7\ \frac{V^2(\alpha)q_0}{(2\pi)^{\alpha-1}}\left[\frac{\gamma_h}{[1+\xi_h^2(\alpha)]^{(\alpha+3)/2}}-\frac{\gamma_e}{[1+\xi_e^2(\alpha)]^{(\alpha+3)/2}}\right]^2, \tag{30}$$

where the phonon wave vector, $|\mathbf{q}|$, is restricted to the range

$$K-\left(K^2-\frac{3E_bM}{2K^2\hbar^2}-\frac{2M\omega_{\mathrm{LO}}}{\hbar}\right)^{1/2} \leqslant q\leqslant K+\left(K^2-\frac{3E_bM}{2K^2\hbar^2}-\frac{2M\omega_{\mathrm{LO}}}{\hbar}\right)^{1/2}, \tag{31}$$

where the exciton energy, E_b is given in Eq. (24).

Using the three-dimensional effective Rydberg energy, R_y, as 3.1 meV for the heavy-hole exciton, $\hbar\omega_{\mathrm{LO}}=36.8$ meV, $\gamma_e=0.3$ and $\gamma_h=0.7$[4] for $GaAs/Al_xGa_{1-x}As$ quantum wells, the linewidths $\Gamma_{1s,1s}$ and $\Gamma_{2p,1s}$ in Eqs. (28) and (30) are calculated for $q_0=2$, 2.5, and 3 in Fig. 5. For selected ranges of q_0 and α, the order-of-

magnitudes of exciton linewidth in GaAs/Al are consistent with available experimental results[32] which show that the excitonic linewidth decreases from 11 to 8 meV as the well width increases from 60 Å to 200 Å.

The linewidths $\Gamma_{1s,1s}$ and $\Gamma_{2p,1s}$ can be seen to be highly sensitive to α. It is to be noted that we have not considered the effects of temperature and other experimental conditions (e.g., interface roughness, excitation intensity) when computing the exciton linewidths. Inclusion of these factors is expected to introduce a change (10–30 %) in our calculated results shown in Fig. 5. The effects of leakage of the excitonic wavefunction into the barrier region on the excitonic linewidths in quantum wells can be predicted from Fig. 4. This behavior has already been observed by Bertolet *et al.*[33] for heterostructures with binary wells.

It may desirable to compare numerical values of the excitonic linewidths obtained here with those of $\Gamma_{1s,1s}$ [Eq. (28)] calculated[6] using an exact two-dimensional exciton-optical-phonon interaction operator and an exciton model based on a variational wave function. Unlike in Fig. 5, $\Gamma_{1s,1s}$ in Ref. 6 was computed only for long-wavelength optical phonons, and hence showed a very slow decrease with the well width (i.e., increasing α values) for GaAs/Al_xGa_{1-x}As quantum wells.

The strong dependence of the excitonic linewidths on α in Fig. 5 suggests that it may be possible to determine empirical values of α from exciton-phonon scattering experiments. As exciton interactions with short-wavelength optical phonons become dominant at higher temperatures ($\geqslant$150 K), one need to also consider non-negligible contributions from ionized donor impurities, exciton-exciton interactions, and well width fluctuations[34] as well. In this regard, the theory developed here is not adequate enough to yield reliable estimates of α from experimental values of the excitonic linewidths and one may need to utilize the methods described in Sec. III B. However at lower temperatures, exciton scattering with acoustic phonons becomes the sole dominant mechanism[35] thus making it easier to relate experimental linewidths with theoretical expressions based on derivation techniques mentioned in this work. One can thus expect to obtain better estimates of α from exciton-phonon scattering experiments at lower temperatures ($\sim$50 K).

V. CONCLUSION

We have derived simple but realistic analytical expressions for the interaction between an exciton and optical phonons for two illustrative cases of $1s\rightarrow 1s$ and $1s\rightarrow 2p$ exciton scattering. The improved interaction operators are derived within the framework of a fractional-dimensional space. The derivation techniques employed here can easily be extended to exciton-deformation potential interaction and piezoelectric interaction involving acoustic phonons[36] as well.

Numerical results of the exciton linewidths in GaAs/Al_xGa_{1-x}As quantum wells predict exciton transition from three-dimensional to quasi-two-dimensional behavior as the well width is decreased. Our results indicate the importance of dimensionality, α, as a critical factor in the interaction of excitons with short-wavelength optical phonons in quasi-two-dimensional systems. Finally, the flexibility of the derived Hamiltonians may be a useful aid to experimentalists in this field.

APPENDIX A

The derivation of Eq. (14) is based on the method employed by Stein and Weiss[19] for the derivation of Eq. (10). The integral is first solved in one-dimensional space using

$$\int_{1\mathrm{D}} y e^{-\pi c y^2} e^{-2\pi i y t} dy = \frac{it}{c^{3/2}} e^{-\pi t^2/c}. \tag{A1}$$

In an αD space we get

$$\frac{1}{|t|} \int_{\alpha D} \mathbf{y}\cdot\mathbf{t}\; e^{-\pi c y^2} e^{-2\pi i \mathbf{y}\cdot\mathbf{t}}\, \mathbf{dy} = \frac{it}{c^{(\alpha+2)/2}}\, e^{-\pi t^2/c} \tag{A2}$$

for vectors $\mathbf{y}$ and $\mathbf{t}$, such that $\mathbf{y}\cdot\mathbf{t}=yt\cos\theta$, θ is a pesudo-angle in the fractional-dimensional space.

Using the relations

$$e^{-2\pi|y|} = \frac{1}{\sqrt{\pi}} \int_0^\infty \frac{e^{-u}}{\sqrt{u}} e^{-\pi^2|y|^2/u} du, \tag{A3}$$

$$\int_0^\infty x^a e^{-bx} dx = \frac{\Gamma[a+1]}{b^{a+1}}, \tag{A4}$$

and Eq. (A2) we get

$$\frac{1}{|t|} \int_{\alpha\mathrm{D}} d\mathbf{y}\, \mathbf{t}\cdot\mathbf{y}\; e^{-2\pi|\mathbf{y}|c} e^{-2\pi i \mathbf{t}\cdot\mathbf{y}} = \frac{\Gamma\left[\frac{\alpha+3}{2}\right]}{\pi^{(\alpha+3)/2}} \frac{ict}{(c^2+t^2)^{(\alpha+3)/2}}. \tag{A5}$$

[1] F. G. Michl, R. Winkler, and U. Rossler, Solid State Commun. **99**, 13 (1996).

[2] S. Schmitt-Rink, D. S. Chemla, and D. A. B. Miller, Adv. Phys. **38**, 89 (1989).

[3] M. Zahler, E. Cohen, J. Salzman, E. Linder, E. Maayan, and L. N. Pfeiffer, Phys. Rev. B **50**, 5305 (1994).

[4] G. Bastard, *Wave Mechanics Applied to Semiconductor Heterostructures* (Les Editions de Physique, France, 1988).

[5] T. Takagahara, Phys. Rev. B **31**, 6552 (1985).

[6] S. Rudin and T. L. Reinecke, Phys. Rev. B **41**, 3017 (1990).

[7] A. Von Lehmen, J. E. Zucker, J. P. Heritage, and D. S. Chemla, Phys. Rev. B **35**, 6479 (1987).

[8] A. Garcia-Cristobal, A. Cantarero, C. Trallero-Giner, and M. Cardona, Phys. Rev. B **49**, 13 430 (1994).

[9] B. Zhang, Y. Shiraki, and R. Ito, J. Phys. Soc. Jpn. **63**, 358 (1994).

[10] G. Q. Hai, F. M. Peeters, and J. T. Devreese, Phys. Rev. B **48**, 4666 (1993).

[11] N. Mori and T. Ando, Phys. Rev. B **40**, 6175 (1989).
[12] J. S. Bhat, B. G. Mulimani, and S. S. Kubakaddi, Phys. Rev. B **49**, 16 459 (1994).
[13] X. F. He, Phys. Rev. B **43**, 2063 (1991).
[14] H. Mathieu, P. Lefebvre, and P. Christol, Phys. Rev. B **46**, 4092 (1992).
[15] P. Lefebvre, P. Christol, and H. Mathieu, Phys. Rev. B **48**, 17 308 (1993).
[16] P. Lefebvre, P. Christol, H. Mathieu, and S. Glutsch, Phys. Rev. B **52**, 5756 (1995).
[17] *Light Scattering in Solids II*, edited by M. Cardona and G. Guntherodt, Topics in Applied Physics Vol. 51 (Springer Verlag, Berlin, 1982).
[18] The proof of the theorem on which Eq. (10) is based was first presented by S. Bochner and K. Chandrasekharan, *Fourier Transforms* (Princeton University Press, 1949).
[19] E. M. Stein and G. Weiss, *Introduction to Fourier Analysis on Euclidean Space* (Princeton University Press, Princeton, NJ, 1975), p. 7.
[20] A. A. Gogolin and E. I. Rashba, Solid State Commun. **19**, 1177 (1976).
[21] D. S. Bulyanitsa, Sov. Phys. Semicond. **4**, 1081 (1971).
[22] D. A. Kleinman, R. C. Miller, and A. C. Gossard, Phys. Rev. B **35**, 664 (1987).
[23] A. J. Shields, M. Cardona, R. Nötzel, and K. Ploog, Phys. Rev. B **46**, 10 490 (1992).
[24] L. Vina, J. M. Calleja, A. Cros, A. Cantarero, T. Beredschot, J. Perenboom, and K. Ploog, Phys. Rev. B **53**, 3975 (1996).
[25] P. Y. Yu, *Optical Properties of Semiconductors*, edited by G. Martinez (Kluwer Academic Publishers, Dordrecht, 1993), p. 65.
[26] G. Oelgart, M. Proctor, D. Martin, F. Morier-Genaud, F.-K. Reinhart, B. Orschel, L. C. Andreani, and H. Rhan, Phys. Rev. B **49**, 10 456 (1994).
[27] L. C. Andreani and A. Pasquarello, Phys. Rev. B **42**, 8928 (1990).
[28] Z. L. Yuan, Z. Y. Xu, Weikun Ge, J. Z. Xu, and B. Z. Zheng, J. Appl. Phys. **79**, 424 (1996).
[29] B. Segall and G. D. Mahan, Phys. Rev. **171**, 935 (1968).
[30] A. Thilagam, J. Lumin. **71**, 245 (1997).
[31] F. Clerot, B. Deveaud, A. Chomette, A. Regreny, and B. Sermage, Phys. Rev. B **41**, 5756 (1990).
[32] Y. Chen, G. P. Kothiyal, J. Singh, and P. K. Bhattacharya, Superlattices Microstruct. **3**, 657 (1987).
[33] D. C. Bertolet, J. K. Hsu, K. M. Lau, E. S. Koteles, and D. Owens, J. Appl. Phys. **64**, 6562 (1988).
[34] J. Lee, E. S. Koteles, and M. O. Vassell, Phys. Rev. B **33**, 5512 (1986).
[35] A. Thilagam and J. Singh, Phys. Rev. B **48**, 4636 (1993).
[36] C. Kittel, *Quantum Theory of Solids* (Wiley, New York, 1963).